Journal of Veterinary Science and Animal Husbandry
Volume 12 | Issue 2
ISSN: 2348-9790

Research Article Open Access

Multiparametric Analysis of the Skin Barrier of C57BL/6J Hairy and SKH1 Hairless Mice

Dorottya Kocsis[1], Fabiola Emilia Kreis[2], András Fülöp[1], Csaba Pongor[1], Anita Báthory-Fülöp[1], Péter Sasvári[2], Barnabás Bánfi[1], Márton Bese Naszlady[1], Kende Lőrincz[3], Roland Csépányi-Kömi[2,#] and Franciska Erdő[1,*,#]

[1]Faculty of Information Technology and Bionics, Pázmány Péter Catholic University, Budapest, Hungary
[2]Department of Physiology, Semmelweis University, Budapest, Hungary
[3]Department of Dermatology, Venerology and Dermatooncology, Semmelweis University, Budapest, Hungary
[#]Franciska Erdő and Roland Csépányi-Kömi contributed equally to this article.

[*]**Corresponding Author:** Franciska Erdő, Faculty of Information Technology and Bionics, Pázmány Péter Catholic University, Budapest, Hungary, Tel.: +36-203541081, E-mail: erdo.franciska@itk.ppke.hu

Citation: Dorottya Kocsis, Fabiola Emilia Kreis, András Fülöp, Csaba Pongor, Anita Báthory-Fülöp et al. (2024) Multiparametric Analysis of the Skin Barrier of C57BL/6J Hairy and SKH1 Hairless Mice, J Vet Sci Ani Husb 12(2): 205

Received Date: October 16, 2024 **Accepted Date:** November 16, 2024 **Published Date:** November 20, 2024

Abstract

Background: In dermatological and pharmaceutical research ex vivo mouse skins are frequently used in topical drug delivery studies and analysis of skin diseases. One part of the experiments reported is carried out in hairless mouse skins, such as SKH1 nude mice, while others prefer the widely validated C57BL/6J hairy mice. However, in-depth characterization of the dermal barrier under healthy conditions has not been performed yet. In the current study tissue morphology, chemical composition, transepidermal water loss, and drug permeability were measured and compared at different anatomical regions in C57BL/6J and SKH1 mice.

Results: The results indicate that skin thickness is higher in nude mice, and consequently, the permeability is lower. The histology revealed that big cysts dominate the dermal layer of SKH1 mouse skin contrary to C57BL/6J. Also on the scanning electron microscopic images remarkable differences were detected in pore density and pore size. The hairy mouse skin was more abundant in lipids (ceramides and cholesterol) and lactate. The protein and urea levels were higher in hairless mice. Mechanical sensitization resulted in a dramatic increase in transepidermal water loss in C57BL/6J mice but caused only a minimal alteration in nude mice.

Conclusion: Based on these observations, it can be concluded that the two mouse models differ greatly. Hence the induction and the observed symptoms of disease models are highly dependent on the strain. This comprehensive dermatological assessment recommends cautious usage of mouse strains in dermatological experiments.

Keywords: C57BL/6J mice, SKH1 nude mice, dermal barrier, skin-on-a-chip, in vitro permeation test, TEWL, confocal Raman spectroscopy

List of Abbreviations: A: adipose cell, AUC: area under the curve, BV: blood vessel, C: ear cartilage, DC: dermal cyst, F: hair follicle, FP: fingerprint region, H&E: hematoxylin-eosin, HR: gene encoding Protein hairless, HWN: high wavenumber, M: muscle, NMF: natural moisturizing factor, PPF: peripheral perfusion fluid, SC: stratum corneum, SEM: scanning electron microscopy, SG: sebaceous glands, TEWL: transepidermal water loss, TS: tape stripping, U: utricle

Background

The integument is the first line of defense against potential harmful insults, acting as a barrier formed by a complex network of physical, chemical, immunological, and microbial agents. The major player of the barrier function is the stratum corneum, which is the uppermost layer of the epidermis. Its structure can be presented as the "brick and mortar" model, where the bricks are the corneocytes, while the "mortar" refers to the adjoining lipids. Corneocytes are terminally differentiated, flattened, enucleated keratinocytes surrounded by cornified envelopes. One part of the envelope contains lipids and proteins such as involucrin, loricin, keratin intermediate filaments, and desmosomal proteins[1]. The external envelope is a multilayered lipid structure forming the „mortar". Its main constituents are ceramides (account for ~50% by weight), cholesterol (25%), and free fatty acids (15%) [2]. Ceramides are waxy lipids, composed of fatty acids and longchain bases with wide structural variations in the number of double bonds, hydroxy groups, and carbon chain length [3]. Skin cholesterol influences the function of keratinocytes and the immune cells, and its content is associated with its level in coronary arteries and the aorta [4–6]. Several other molecules play crucial roles in the formation of the chemical barrier. Natural moisturizing factor (NMF) is essential for appropriate stratum corneum hydration, barrier homeostasis, desquamation, and plasticity [7]. It is formed by lactate, proteins, urea, sugar, and inorganic ions such as potassium and magnesium ions. Lactate provides anti-aging and keratolytic action and stabilizes the pH, which is important in the formation of acidic skin surface that restricts bacterial colonization [8]. Proteins and urea also have moisturizing, rehydrating, and anti-aging effects. Urea is a hygroscopic molecule that is essential for the hydration and integrity of the stratum corneum. Urea improves skin barrier function including antimicrobial defense and regulates keratinocyte proliferation. Urea is widely used as a moisturizer and keratolytic agent [9]. Moreover, the water content is a key aspect of the skin that influences its physical and mechanical properties. Hydration leads to changes in the molecular arrangement of the peptides in the keratin filaments within the stratum corneum [10].

This complex barrier is dysfunctional in several dermatological diseases, which are a major problem worldwide. Hence the design and development of effective therapeutic strategies is essential. In this research, animal experiments play an important role in pharmaceutical, pharmacological, and dermatological studies. Animal models are important in dermatological research because they can help to understand the causes, mechanisms, and treatments of various skin diseases affecting humans and animals. Rodent models can mimic the symptoms, pathology, and response to therapy of human skin diseases such as psoriasis, atopic dermatitis, acne, vitiligo, melanoma, and other skin disorders [11]. However, using laboratory animals also has certain limitations and challenges, such as differences in anatomy, physiology, genetics, and immune systems in various animals strains and in animal-human relations.

C57BL/6 is the most widely used inbred mouse strain because these mice breed well, are long-lived, and allow the expression of most mutations [12]. However, the use of C57BL/6 mice also has its drawbacks: a low susceptibility to tumors, development of severe and progressive hearing loss, and demonstrating an orientation toward T helper1 responses [13, 14]. Being a hairy strain, shaving and depilation of the hair before the dermatological investigation is a prerequisite. To provide an appropriate hair removal method and maintain animal welfare, He and co-workers compared four commonly used depilation methods--namely, scissors shearing, electric shaving, depilatory cream, and sodium sulfide, and concluded that the electric shaving method was more convenient and safer than the others, suggesting it as the best choice for preoperative depilation [15].

There are different hairless mice, but in spite of the outbred status and the not fully characterized genetic background, the

SKH1 stock is one of the most widely used nude mouse models in dermatologic research [16]. These animals carry an autosomal recessive hypomorphic mutation called *hr* in the gene *Hairless* (*Hr*). The encoded Hr protein is highly expressed in the skin and brain and acts as a transcriptional co-repressor for multiple nuclear receptors, such as the thyroid hormone receptor, retinoic acid receptor, and the vitamin D receptor [17]. The absence of the repressor protein HR in *hr* mice alters the transcription of gene products that function in keratinocyte differentiation and immune cell proliferation [17]. The first hair coat develops normally, but at 2 weeks after birth, a quick hair loss begins at the eyelids and proceeds caudally, with a sharp boundary between hairless and haired areas. By about 3 weeks of age, the animals are completely hairless except for a few vibrissae, which are shed repeatedly, becoming more abnormal and sparser with each regrowth [16]. These unpigmented and immunocompetent mice allow easy manipulation and examination of the skin, application of topical agents, exposure to UV radiation, and easy visualization of the cutaneous reaction. Wound healing, acute photobiologic responses, and skin carcinogenesis have been extensively studied in SKH1 mice [16]

Although both the C57BL/6J and SKH1 mice are widely used as dermatological model animals, the characterization of the dermal barrier under healthy conditions has not been performed yet. Our study focused on the physical and chemical barrier and aimed to compare the skin of C57BL/6J and SKH1 mice measuring transepidermal water loss, in vitro permeation capability for a model drug, and analysing the chemical composition. Since different dermatological models use different anatomical regions, the dorsal, abdominal, and auricular skins were characterized. The dorsal skin is frequently treated in psoriasiform dermatitis models [18, 19], the abdominal area is subjected to the induction of the allergic contact dermatitis [20, 21], and the ears are used in the sensitization phase in the same model.

The practical implications of studying the dermatological characteristics of hairy and nude mice are the optimization of different drug and cosmetic formulations in regard of the degree and kinetics of skin absorption and bioavailability of active ingredients and also using them as an appropriate disease models. The significant differences between the hairy and hairless mouse skins revealed by the current assessment recommend their cautious usage in translational experiments.

Materials and Methods

The aim of this study was to compare the dermatological properties of two widely utilized mouse strains with a multiparametric approach to help future model selection in experimental skin research.

Animals

The hairy, wild-type C57BL/6J strain and the hairless SKH1 mouse stock on a BALB/c background were purchased from Charles River Laboratories (Germany) [16]. Animals were bred and housed individually (Tecniplast, Buguggiate, Italy) in a conventional animal facility. Animals were fed standard chow ad libitum and had unlimited access to water. Age- and gender-matched animals were used for the experiments. All experiments were approved by the Animal Experimentation Review Board of Semmelweis University and the Government Office for Pest County (Hungary) (Ethical approval number: PE/EA/1967-2/2017). Three hairy and three nude mice were used for the experiments.

Skin Preparation

Considering the previous findings of He and co-workers on convenient and safe depilation methods [15], the C57/BL6 mice were shaved with an electric shaver and depilated (X-Epil, Aveola Kft., Budapest, Hungary) for 5 minutes under isoflurane anesthesia. The skin was then washed and wiped dry. All the C57BL/6J and SKH1 mice were overanesthetized and the full-thickness abdominal, dorsal, and auricular skin was quickly excised. The subcutaneous adipose tissue was gently removed. Intact skin was used for histology, scanning electron microscopy, Raman spectroscopy, and for the transepidermal water loss (TEWL) mea-

surements. The skins which were subjected to 10 times tape stripping (10TS) with an adhesive tape (BSN Medical GmbH, Hamburg, Germany) were used for permeability study. The double-fold skin thickness was measured with a micrometer (Asimeto, Budapest, Hungary) with 0.1 mm accuracy. The ears were not subjected to any hair removal or mechanical sensitization.

Excised samples were wrapped in aluminum foil and stored at -80°C. In the case of the permeability studies, skins were thawed for 30 minutes at room temperature. At Raman spectroscopy and TEWL, the skin samples were thawed on the previous day and stored at 4°C overnight. The consistency of the ex vivo tissue samples was sufficiently preserved for Raman spectroscopy, TEWL measurement and drug delivery studies as it was proved by unpublished pilot experiments which compared freshly prepared and frozen and thawed samples.

Scanning Electron Microscopy (SEM)

Samples were fixed and dehydrated for analysis through scanning electron microscopy as described earlier [19].

The SEM-obtained images were analyzed using image processing methods to find the characteristics that help to distinguish between C57BL/6J and SKH1 skins.

Based on the intensity values, a threshold was applied to the images to generate binary pictures from grayscale images. Object search and counting were performed according to our previous paper [19]. Suzuki's Contour tracing algorithm was used to find the contours [22]. Two parameters were used, N_G (number of gaps) and N_{PC} (number of pixels in cells) to separate the different types of images.

Skin Barrier Function

Transepidermal water loss measurements were performed with the condenser-chamber device Vapometer® (Delfin Technologies Ltd., Kuopio, Finnland) according to the instructions of the manufacturer.

Skin permeability testing in microfluidic diffusion chamber

The skin permeability tests were performed in an in-house developed skin-on-a-chip designed for in vitro permeation tests [23–25]. It contains a donor and a receptor chamber, while the skin is placed in between these two units allowing a penetration surface for the active ingredient. The donor chamber was filled with a 2% caffeine cream. Caffeine is a widely used hydrophilic model substance in in vitro release and permeation studies using different synthetic membranes and ex vivo animal or human skins [26, 27]. The receptor chamber contained peripheral perfusion fluid (PPF, consisting of 147 mM NaCl, 4 mM KCl, and 2.3 mM $CaCl_2$, all substances acquired from Sigma-Hungary Kft., Budapest, Hungary). The perfusion flow rate was 4 µL/min. The abdominal, dorsal, and auricular skins were placed between the donor and receptor compartments and had a diffusion surface of 0.5 cm^2. Samples were collected every 30 min for 5 hours and stored at -80°C until bioanalysis.

Bioanalysis of Caffeine in Perfusate Samples

The bioanalysis was performed with a spectrophotometer (NanoDrop™ 2000, Thermo Scientific, Budapest, Hungary). The absorption maximum of caffeine was detected at 272 nm.

Full-Thickness Skin Histology

Four µm thick hematoxylin-eosin (H&E) stained slides were produced by standard histologic procedure from paraffin-embedded blocks. The slides were scanned by 3DHistech Panoramic 250 Flash III scanner (3DHISTECH Ltd, Budapest, Hungary). Measures were performed by CaseViewer (3DHISTECH Ltd, Budapest, Hungary).

Skin Composition Analysis by Confocal Raman Spectroscopy

Confocal Raman spectroscopy analysis was performed with GEN-2 SCA Skin Composition Analyzer (River D- International BV, Rotterdam, The Netherlands) equipped with two incorporated lasers. The method was described earlier by Kocsis et al.[28].

For each skin sample, 7 areas were recorded using depth profiling (z-profiling) for both fingerprint (FP) and high wavenumber (HWN) regions. The FP z-profilings were carried out with a 5 s exposure time and 3 μm steps up to 39 μm depth. For the HWN measurements, 5 s exposure time with 3 μm steps until 20 μm and 6 μm steps between 20 μm and 68 μm as final depths were used for z-profiling.

Skin components profiles (ceramides, fatty acids, cholesterol, lactate (pH=4), proteins, urea, water) were calculated using the SkinTools 3 analysis software (RiverD International B.V., version 3.3.201202, Rotterdam, The Netherlands) according to the previous work of Caspers et al.[29].

Statistical Analysis

All data were analyzed and plotted using GraphPad Prism 9.5.0 Software (Boston, MA, USA). The comparison of experimental groups was conducted with Student t-test (2,2) or two-way ANOVA. Šídák or Tukey Post Hoc test was used for multiple comparisons. P values <0.05 were considered statistically significant.

Results

Body Weight and Skin Thickness at Various Anatomical Regions

The averaged body weights (Table 1) of C57BL/6J and SKH1 mice were within the standard ranges as shown in the public data of the Charles River Laboratories [30, 31]. The weights of the SKH1 nude mice were significantly higher than that of the C57BL/6J animals at the same age.

The SKH1 mouse skin was 1.18-1.19 times thicker than the C57BL/6J mouse skin in the abdominal and dorsal regions, whereas the ear was found to be 1.57 times thicker (**Table 1**) in SKH1 mice.

Table 1: Comparison of body weight and skin thickness of C57BL/6J and SKH1 mice (means ±SE, n=3)

Parameter	C57BL/6J	SKH1	t- test (2,2)
Age (days)	94	100	-
Body weight (g)	19.00±0.58	26.00±0.58	p=0.001
Ear thickness (mm)	0.2617±0.0049	0.41±0.0286	p=0.014
Ear weight (g)	0.02828±0.00036	0.04507±0.004814	p=0.046
Abdominal skin thickness (mm)	0.4486±0.0383	0.5283±0.0106	p=0.176
Dorsal skin thickness (mm)	0.6083±0.0083	0.7233±0.0098	p=0.002

Superficial Evaluation of Skin Samples from Different Anatomical Regions by Scanning Electron Microscopy (SEM), and Image Analysis

The surface of the skin preparations excised from C57BL/6J and SKH1 mice was studied by scanning electron microscopy. The auricular, abdominal, and dorsal regions were evaluated and on abdominal and dorsal skins two conditions were compared (0TS – intact tissue without mechanical sensitization and 10TS). Four skins were used in each group. Representative pictures and evaluation of low-power (300x) SEM images are shown in Figure 1.

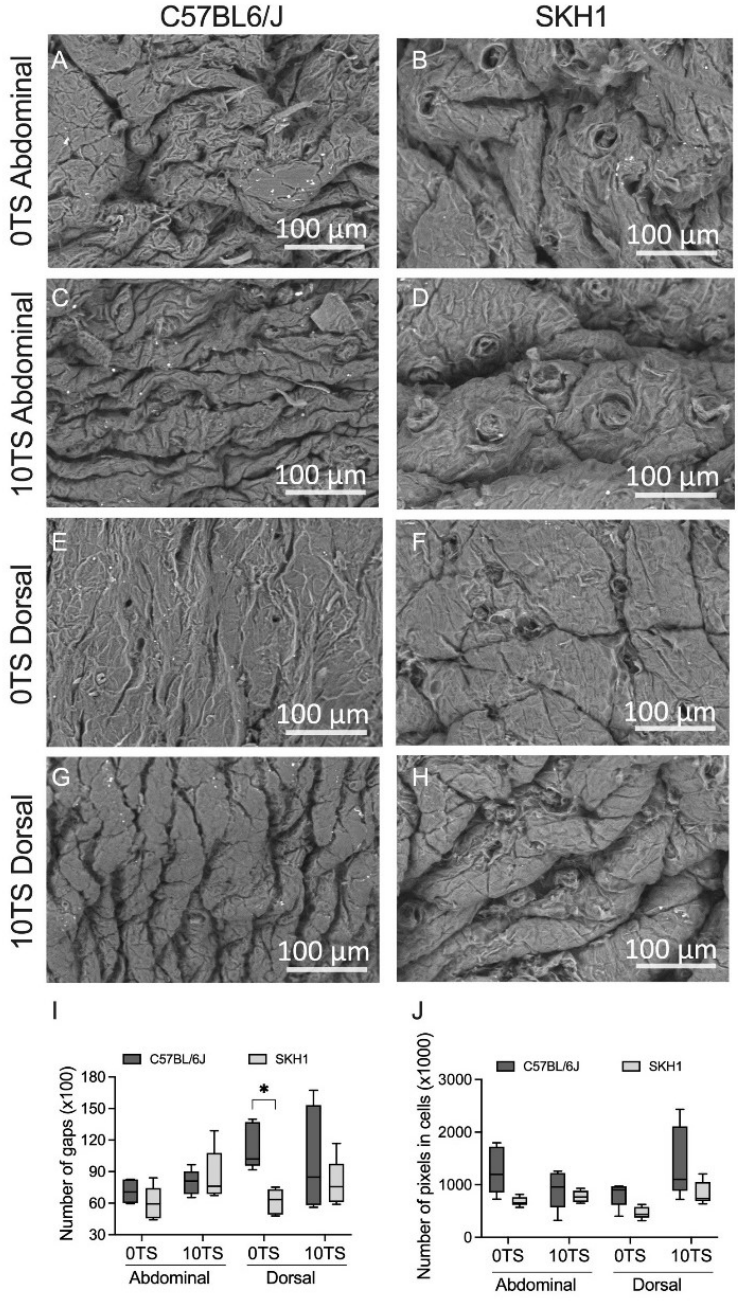

Figure 1: Representative low-power scanning electron microscopic images of C57Bl/6J and SKH1 mouse skins. Panel (A and B) abdominal area without mechanical sensitization, panel (C and D) abdominal area with 10 tape strippings, panel (E and F) dorsal area without mechanical sensitization, panel (G and H) dorsal area with 10 tape strippings, panel (I) image analysis of SEM pictures - number of gaps, and panel (J) image analysis of SEM pictures - number of pixels in cell bodies. (Medians and min/max values are presented in boxplots, n=4/group, *: $p<0.05$).

The squamous, flat corneocytes were well-demarcated in the auricular tissues in C57BL/6J mice, and the cell borders were visible also in nude mice. The distinctive utriculi were present in the SKH1 mouse ear. The abdominal skin surface was wrinkled in the intact C57BL/6J mouse and became more folded after removal of the superficial corneocytes (Figure 1 A,C). In hairless mice, the pore size and density were quite large on the abdominal skin surface, and many degenerative hair follicles were present both in the intact and in the sensitized tissues (Figure 1 B,D). No significant morphological differences could be seen after 10TS in the nude mouse abdominal skin. The dorsal skins seemed to be more rugous and wrinkled after 10TS both in the hairy and hairless mice compared to the intact surface (Figure 1 E,F,G,H). Large pores were also observable in the dorsal stratum corneum in SKH1 mouse skin (Figure 1 F,H). The computer-aided image analysis showed that the both the number of gaps (especially in the dorsal intact skins) and the area of scaly cells were higher in the C57BL/6J strain (Figure 1 I,J).

Morphological Analysis of Skin Samples Taken from Different Anatomical Regions

The hair follicles (F) with connecting sebaceous glands (SG) were well formed in C57BL/6J mice. Adipose cells (A) and the cutaneous muscle layer were also visible (Figure 2 A,C,E). Stratum corneum (SC) forms the outermost layer of the skin and in SKH1 mice it is abundant in the opening of the utriculi (U), which arise from the infundibulum of the hair shaft forming ampuliform structures lined by hyperkeratotic epithelium. Here hypertrophic sebaceous glands could be noted (Figure 2 D). In hairless mice, large multicellular dermal cysts (DC) dominated the deep dermis not connected to the overlying epidermis (Figure 2 B,D,F), and were lined by keratinized epithelium. The DCs might have a hair bulb origin, where the progenitor cells cannot properly undergo the sebaceous gland differentiation [16].

Adipose cells were present in a considerable number in the hypodermal layer. Ear cartilage (C) separated the interior and exterior skins in Figure 2 E and F. Thicker stratum corneum could be seen in SKH1 mouse skin, which extends into the utriculi (Figure 2 B,D, F). Sebaceous glands were especially enlarged compared to the size of the follicles. DCs were present in the ear region as well.

In the abdominal region, a normal skin structure could be observed in C57BL/6J mice (Figure 2A). The epidermis was thin; keratinocytes were located superficially in the basal cell layer. Basophilic staining in the basal cell layer was prominent. Below the epidermis, the eosinophilic staining of the connective tissue made the dermis distinguishable. Embedded into this layer secreting sebaceous glands could be seen, connecting to hair follicles. From below, the dermis was bounded by the adipose tissue. The cutaneous muscle layer, also called the panniculus carnosus, could be seen.

The skin of the SKH1 mice showed multiple visible abnormalities (Figure 2 B) irregular hair follicles, dermal cysts, and enlargement of the sebaceous glands. Pore-like structures (utriculi) were lined by hyperkeratotic epithelial cells [16], which had eosinophilic staining. They connected the follicles to the skin surface. Large dermal cysts with epithelial lining dominated the dermal layer and were not connected to the epidermis. Compared to the abdominal subcutaneous adipose tissue the dorsal hypodermis was more abundant both in C56BL/6J and SKH1 mice (Figure 2 C,D). In SKH1 mice DCs and utriculi were also present in the dorsal skin (Figure 2 D).

In the ears, cartilage separated the interior and exterior skins on the cross-sectional images (Figure 2 E,F). Compared to other anatomical regions the dermis layer was visibly thinner. The dermis was more vascularized. In SKH1 mice skin utriculi, enlarged sebaceous glands and dermal cysts could be found even in the auricular region (Figure 2 F).

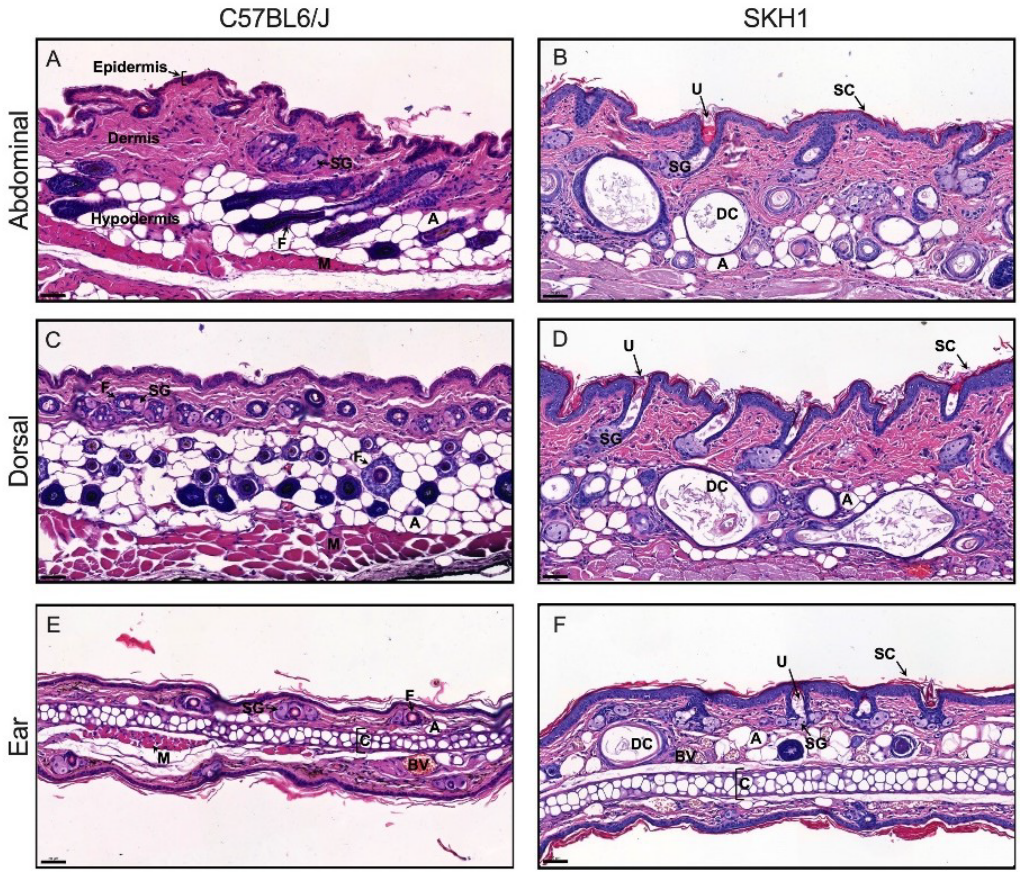

Figure 2: Representative histological cross sections of intact skin samples from C57BL/6J (Panels A,C,E) and SKH1 (Panels B,D,F) mice, 20x magnification. The abdominal (Panels A,B) and dorsal (Panels C,D) regions and the ear tissues (Panels E,F) were sectioned and stained with H&E staining. The three layers of the skin are marked in panel A (epidermis, dermis, and hypodermis). F: hair follicles, SG: sebaceous glands, SC: Stratum corneum, U: Utriculi, DC: dermal cysts, A: adipose cells, M: cutaneous muscle layer, C: ear cartilage, BV: blood vessel. Scale bar is 50 μm.

Evaluation of Skin Composition in C57BL/6J and SKH1 Mice

For analyzing the chemical composition of hairy and nude mouse skins (abdominal and dorsal) six components were selected and detected by confocal Raman spectroscopy at different depths of the intact epidermis. As is seen in Figures 3 A, B, and D, E, the C57BL/6J mouse skins were more abundant in lipid components (ceramides and cholesterol) on the surface, which can be related to the hair growth and active function of sebaceous glands at the root of the hair follicles. But in the deeper layers (from 12-40 μm) the hairless skins were richer in cholesterol. With Raman spectroscopic measurement, we can examine the upper 40-micrometer layer of the epidermis. With age, the properties of this layer and the dermis change the most (e.g. decreasing water, collagen, and elastin contents). Thus, the differences in body weight, which result from the thickness of the subcutaneous adipose tissue, do not play a significant role in the epidermal composition. Therefore, from our point of view, age-related changes in skin structure (primarily in the epidermis and dermis) are more important than differences in the subcutaneous fat layer. Lactate levels were higher in the C57BL/6J mice both in the abdominal and the dorsal skins to ensure the balanced pH of the hairy skin. The water content was higher in the hairy animals only in the abdominal skin (Figure 3 G,H,J,K). The levels of urea were higher in nude mice but only in the deeper layers (12 – 40 μm) (Figure 3 M,N), while the protein contents were very close and ran parallel in the two strains (Figure 3 P,Q). Using the cumulative mass - skin depth profiles, AUC values were calculated. The AUC bar graphs showed higher total lipid content (ceramides, fatty acids, and cholesterol) in the epidermis of SKH1 mice (the only exception was ceramide in the abdominal skins), although the surface layers were more abundant in lipids in

C57BL/6J strain (Figure 3 C,F). Both lactate and total water content were higher in black(?) mice if the whole 40 ⊠m skin thickness is regarded (Figure 3 I,L). Urea was elevated in hairless mice mainly in the deeper skin layers, compared to the blackmice (Figure 3 O). The protein contents were comparable in the two strains but the nude mice showed elevated protein levels if the full thickness of the epidermis is regarded (Figure 3 R). For a comparison of the composition of the three anatomical regions: abdominal, dorsal, and auricular in the same plots, see Figure S1. The composition of the ear tissues in C57BL/6J and SKH1 mice is presented separately in Figure S1.

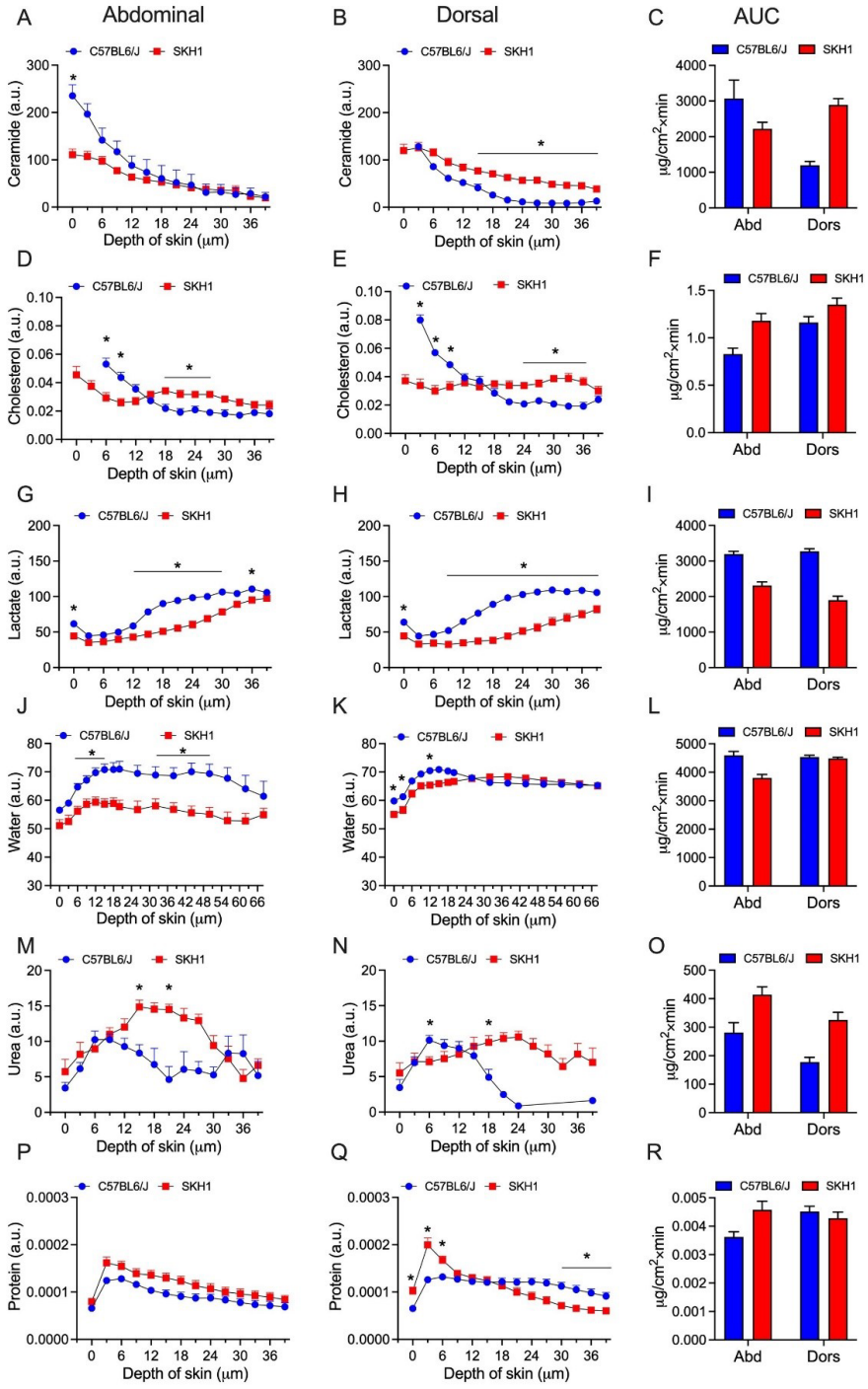

Figure 3: Chemical components of excised skins from C57BL/6J and SKH1 mice. Abdominal (Panels A,D,G,J,M,P) and dorsal (Panels B,E,H,K,N,Q) regions were analyzed. AUC values were determined from the line graphs (Panels C,F,I,L,O,R). The study was performed using confocal Raman microspectroscopy. n=3 skins/strain were analyzed on 7 different sites of the tissues at each z-profile. Means ±SE are presented. *:p<0.05

Transepidermal Water Loss for Skin Barrier Function

Transepidermal water loss was measured as an indicator of barrier impairment. Increased TEWL indicates skin barrier damage [32–34]. The intact (0TS) C57BL/6J and SKH1 skins have similar TEWL values indicating that the shaving did not significantly destroy the barrier. In C57BL/6J mice, the TEWL on the intact skins was similar on the abdominal and dorsal surfaces (7.18±0.93 g/m^{2}h, 5.03±1.18 g/m^{2}h, respectively), whereas both differed significantly from the 10TS samples (35.17±0.60 g/m^{2}h, 35.50±0.67 g/m^{2}h, on abdominal and dorsal samples) (Figure 4 E, F).

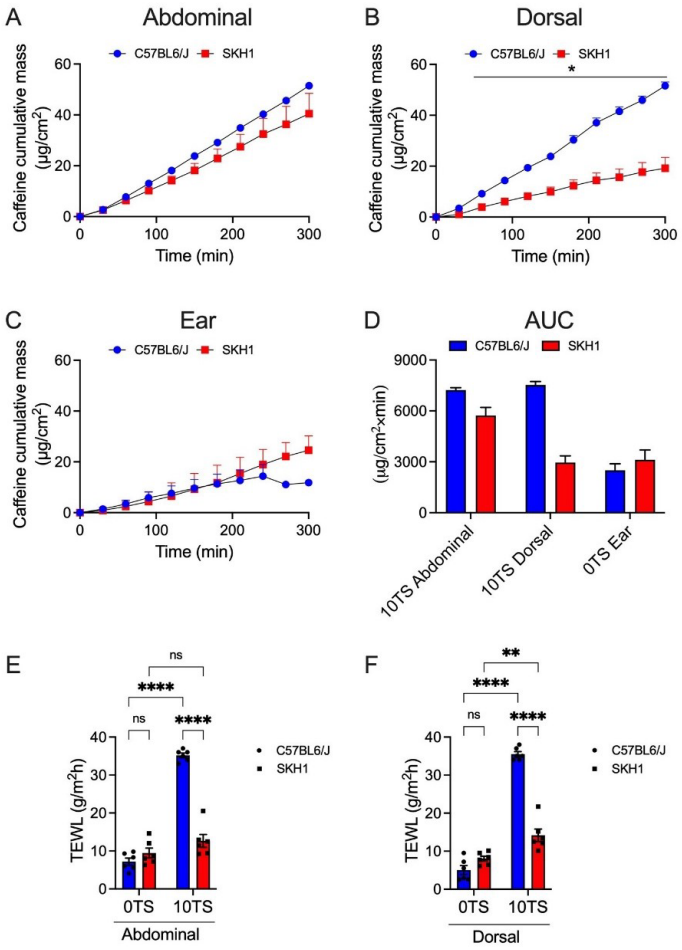

Figure 4: Skin permeability and barrier function on C57BL/6J and SKH1 mouse skins. Caffeine penetration from 2% cream formulation throught the (A) abdominal skin, (B) dorsal skin, (C) auricular skin and (D) Area under the cumulative mass-time curves (AUC). Skin barrier function in (E) abdominal and (F) dorsal region of the skin of C57BL/6J and SKH1 mice. The mechanical sensitization (10 TS) was significantly more effective in C57BL/6J than in the SKH1 mice. Means ± SE, n=3. *: p<0.05, **: p<0.01, ****: p<0.0001.

These differences were much less prevalent in SKH1 mice. It might be explained as a consequence of the skin thickness, since the SKH1 mice have thicker and structurally more compact integuments, i.e., the 10TS could not destroy the barrier function to the same degree, as in the C57BL/6J animals.

In Vitro Permeation Test

The cumulative mass-time profiles of caffeine absorption through the barrier in different ex vivo mouse skin samples are presented in Figure 4. The penetration kinetics of caffeine through the SKH1 dorsal and abdominal skins was slower with lower

C_{max} levels than that of the C57BL/6J (Figure 4 A, B & D). The result is consistent with the skin thickness measurements. However, comparable absorption characteristics could not be found in the ear tissues (Figure 4 C), where the C57BL/6J and SKH1 samples showed similar penetration profiles in the first 180 min (Figure 4 C). C57BL/6J mouse ears did not undergo any depilation process, therefore some hairs remained on the surface, which might interfere with the transdermal penetration. For a comparison of the three anatomical regions: abdominal, dorsal, and auricular skins, in the same plots, see S3 Figure.

Discussion

To mimic human skin disorders and to develop effective topical and transdermal drugs, rodents are extensively used in dermatological and pharmaceutical research [11]. As ex vivo studies are frequently conducted in excised rodent skins, this article focused on the comparative dermatological analysis of the skin of hairy C57BL/6J and hairless SKH1 mice.

Schaffer and co-workers compared the humoral and cellular immune function of the SKH1 and C57BL/6 mice aiming to determine whether the hypomorphic mutation in the Hairless gene would or would not affect the immune competence [17]. They found that blood counts, immunoglobulin levels, and CD4+ and CD8+ T cells were comparable between the SKH1 and the C57BL/6 strain [17]. On examination of T cell subsets, statistically significant differences in naive T cells and memory T cells were detected. However, the numerical differences did not result in altered T cell functional response to antigen re-challenge in a lymph node cell proliferative assay [17]. Jain et al. studied the nitrogen mustard-induced cutaneous effects in C57BL/6 and SKH-1 mice [35]. They found a significant increase in epidermal thickness, incidence of microvesication, cell proliferation, apoptotic cell death, inflammatory cells (neutrophils, macrophages, mast cells) and myeloperoxidase activity in the skin in both mouse strains after exposure. However, the SKH1 mice showed a more prominent increase in epidermal thickness, and macrophages and mast cell infiltration relative to what was seen in C57BL/6 mice. They concluded that both studied mouse groups are useful tools for screening and identification of effective therapies for the treatment of skin injuries caused by nitrogen-mustard. A recent study compared the two mouse strains in reaction after dermal xxposure to vesicating nettle agent phosgene oxime, a chemical weapon [36]. Konger et al. compared the acute UV-induced photoresponse between the SKH1 mice and an immunocompetent, hairless, albino C57BL/6J congenic mouse line [B6.*Cg-Tyrc-2JHr*^{hr}/J] [37]. Histologically, the skin of the congenic mice was indistinguishable from that of SKH1 mice. All the mice exhibited a reduction in hypodermal adipose tissue, epidermal thickening, the presence of utricles and dermal cystic structures, and dermal granulomas. However, the congenic C57BL/6 mice exhibited a more robust delayed sunburn reaction, with an increase in epidermal erosion, scab formation, myeloperoxidase activity, and aberrant proliferative response, suggesting that the congenic mice are more suitable for photobiology experiments [37].

As discussed above, there are literature data on the immunological comparison of C57BL/6 and SKH1 mice, however, the dermatological comparison, in relation to the physical and chemical skin barrier has not been performed yet. Therefore, this study was focused on the physical parameters, characterizing the superficial and the cross sectional tissue morphology. The chemical composition of epidermis in terms of the substances important in the barrier formation was also determined at different skin depths. Finally, the functionality of the barrier, by measurement of transepidermal water loss and in vitro permeability assay were conducted.

Regarding the physical parameters, similar changes were observed in SKH1 nude mouse skin as have been described in other hairless strains in the literature. Köpf-Maier, Mboneko, and Merker were some of the first researchers who studied the surface of the skin and the hairs of hairy (NMRI) and nude (NMRI, nu/nu) mice using electron microscopy [38]. These morphological studies revealed that athymic, macroscopically nude mice are not completely hairless, but have about the same number of hair bulbs containing impaired, short, bent hair shafts [38]. Similarly, the abnormal hair structures could be observed in the SKH1 mice in our study as well. Observing the hematoxylin-eosin-stained samples, several morphological degenerations could be

seen in the nude mouse skin, including the presence of utriculi, degenerative sebaceous glands at the hair follicles, and large dermal cysts. Similar to our results, Massironi et al. found cystic formations (i.e. utricles) and dermal cysts in the mutant hairless USP mouse strain. Except for these, no qualitative differences were found during the development of the skin of BALB/c and the mutant nude mice [39]. Also, the thickness of the dermis became significantly larger with aging in the nude mutant compared to the wild-type BALB/c mice [39]. Immunohistochemical staining for fibronectin and laminin did not show differences and the mast cells and macrophages positive for HAM 56 antibodies were also observed in both mouse strains [39].

As for the chemical composition of the epidermis, it can be concluded, that the surface layers of the hairy mouse skin were more lipophylic, but deeper (at 10-12 μm-40 μm); hairless skin was more abundant in lipid components. These results suggest that the penetration of lipophilic topical drugs and formulations to the superficial skin can be more intensive in blackmice, while the transdermal delivery across the skin barrier seems to be more efficient in the SKH1 strain. Lactate and water levels were higher in C57BL/6J mice indicating a more balanced milieu in the hairy mouse skin; while the NMF components were more abundant in SKH1 mouse epidermis. As the defending function of the hair against dehydration is not present in nude mice, the higher level of moisturizing factors performs this protection in the viable epidermis.

In vitro permeation tests are commonly used to evaluate the transdermal penetration of topical/transdermal dermatological products. Permeability is an indicator of barrier function, therefore in this study the absorption of a drug containing cream formulation was tested in both strains. As a model drug caffeine was chosen because it is a widely used additive in dermatopharmacological products and also it is a hydrophilic model compound. Its pharmakokinetic properties are well-characterized [40] as numerous research groups are using it for comparing different models, including artificial membranes and reconstructed human epidermis [28, 41, 42]. Higher penetration rate on the C57BL/6J mouse skin was observed in the current study, which is in correspondence with the previous results on skin thickness, SEM, and TEWL measurements. Moreover, the hydrophilic caffeine permeates the skin partly in transappendageal route, via the hair follicles,[43] which are degenerative in SKH1 mice.

These results indicate, that despite the hair-removal procedure, the C57BL/6J strain seems to be more beneficial in drug absorption studies, due to the more physiological skin structure and higher degree of the drug penetration that can be achieved. This makes possible to reach the detection limit of the bioanalytical method and to determine the frequently very low drug concentrations in the subcutis.

Conclusions

In summary, based on the results, it can be concluded that the defensive role of the dermal barrier of SKH1 mice is more prominent than that of the C57BL/6J mice. This observation is supported by the fact that the hair itself promotes the barrier function of the skin in C57Bl/6J mice. The skin, including the epidermis, is thicker in nude mice, and degenerative elements like dermal cysts and utriculi are also present in this skin, which could be quantified in the histological sections. On the SEM captures, the number of gaps between the cells increased more after tape stripping in the C57BL/6J than in the SKH1 mice, which also corresponds to the TEWL values, which showed a greater increase in the C57BL/6J mice after repeated mechanical sensitization. In accordance with all these findings, the in vitro permeation test also confirmed the stronger barrier function and the weaker permeability of the skin of SKH1 mice.

Overall, before selecting a mouse strain for skin research (e.g. for dermatological studies, or for pharmaceutical development and for translational pharmacological investigations), the physico-chemical properties of the topical/transdermal test substances, the characteristics of the formulations applied and the scientific goal of the study should all be taken into account. Although there are some practical reasons why nude animals are more beneficial in dermatological research (no depilation needed, good visibility, direct study of the skin inflammation, and the effect of UV radiation), some disease models work better in

C57BL/6J mice. Earlier some dermatological disease models (psoriasis, allergic contact dermatitis, wound healing) were also compared in these two strains in our laboratory (unpublished data) and serious differences have been detected in the responsiveness to the chemical, immunological or physical stimuli. The findings of this article, and the previously reported data on the dermatological assessment of model animals and artificial tissue [28, 44, 45] should all be carefully considered when planning and comparing dermatological studies in rodents and reveal the high potential of utilization of these strains in pharmaceutical developments.

Availability of Data

The raw data are available from the authors for request.

Competing Interest

The authors declare no conflict of interest.

Funding

This work was supported by the TKP2021-EGA-42 grant funded by the Ministry of Innovation and Technology, Hungary with support from the National Research Development and Innovation Fund under the TKP2021 programme.

Authors' contribution

Conceptualization FE, RCs-K, KL; methodology DK, FEK, CsP, AF, ABF; software AF, FEK, MBN, RCs-K; validation FE, RCs-K, MBN; investigation DK, BB, FEK, CsP, AF; resources FE, RCs-K; data curation DK, FEK, RCs-K; writing—original draft preparation FE, DK, RCs-K,.AF; writing—review and editing RCs-K, KL, FEK, DK, BB; visualization FEK, DK, RCs-K; supervision FE, RCs-K, LK; funding acquisition FE, RCs-K. All authors have read and agreed to the published version of the manuscript.

Acknowledgements

The authors are grateful to all members of NMNS (EA 6295 Nanomédicaments et NanoSondes) Laboratory of the University of Tours for giving continuous support to this research and providing the RiverD confocal Raman system for the experiments. We are also grateful to Dr. László Báthory-Fülöp for the technical support related to histology and to Mr and Mrs Kovach for English polishing.

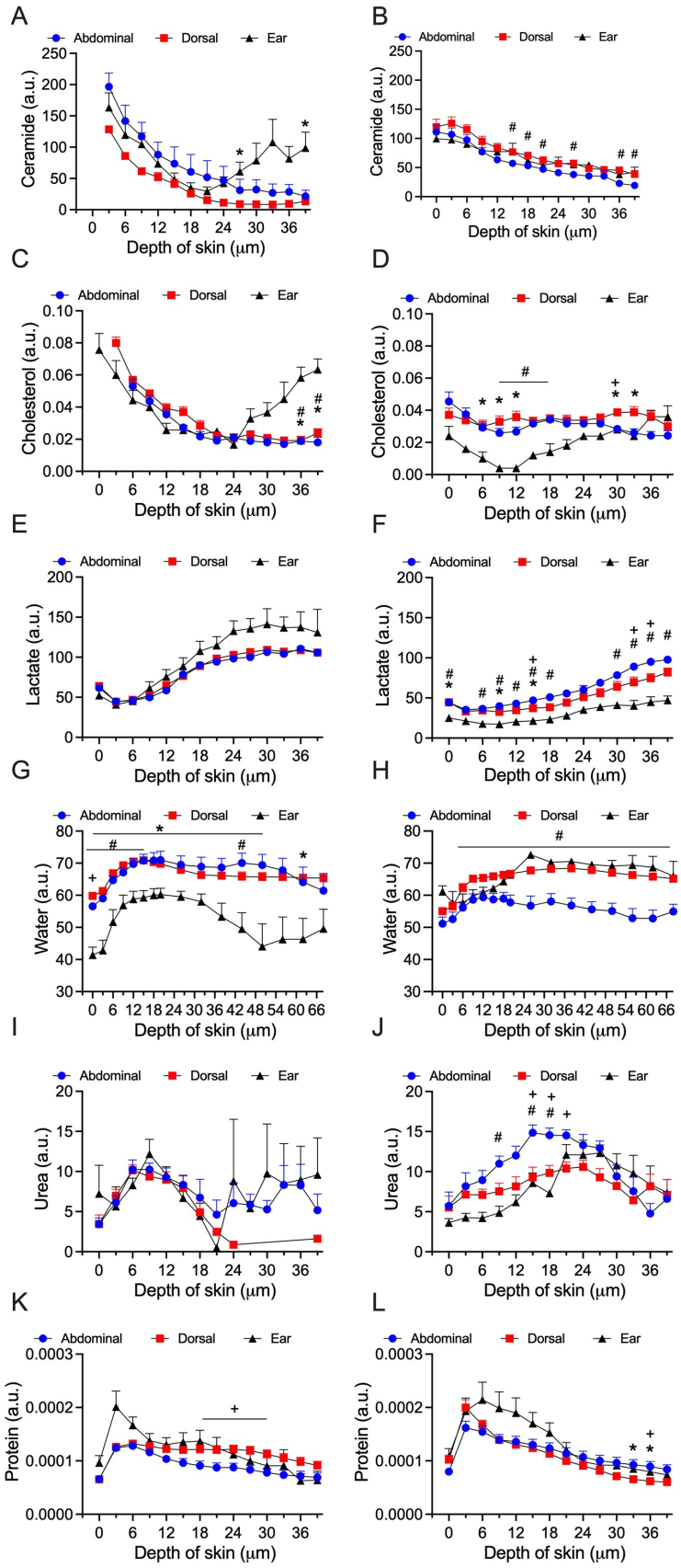

S1 Figure: Skin components at different epidermal layers of three anatomical regions (A,C,E,G,I,K) in C57BL/6J mice, (B,D,F,H,J,L) in SKH1 mice, measured by confocal Raman spectroscopy

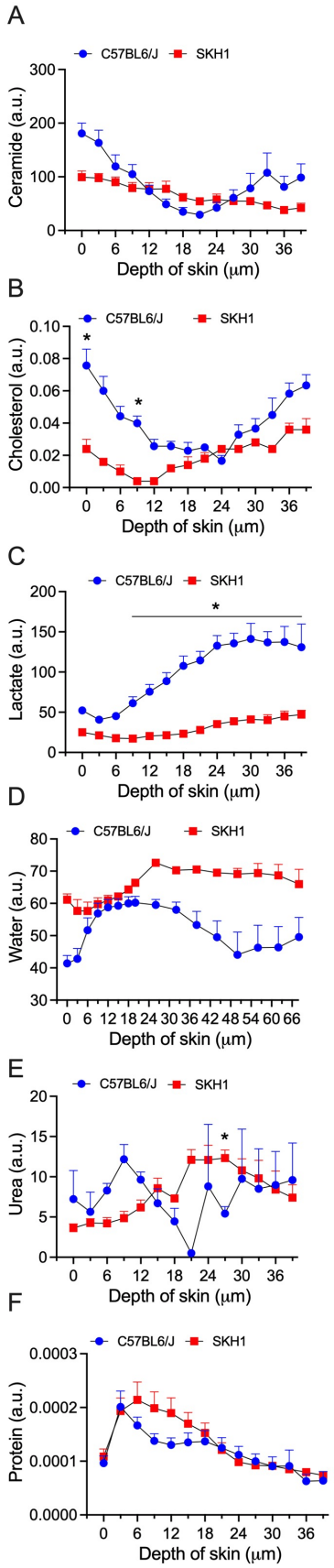

S2 Figure: Comparison of the auricular skin components at different epidermal layers in C57BL/6J and SKH1 mice, measured by confocal Raman spectroscopy

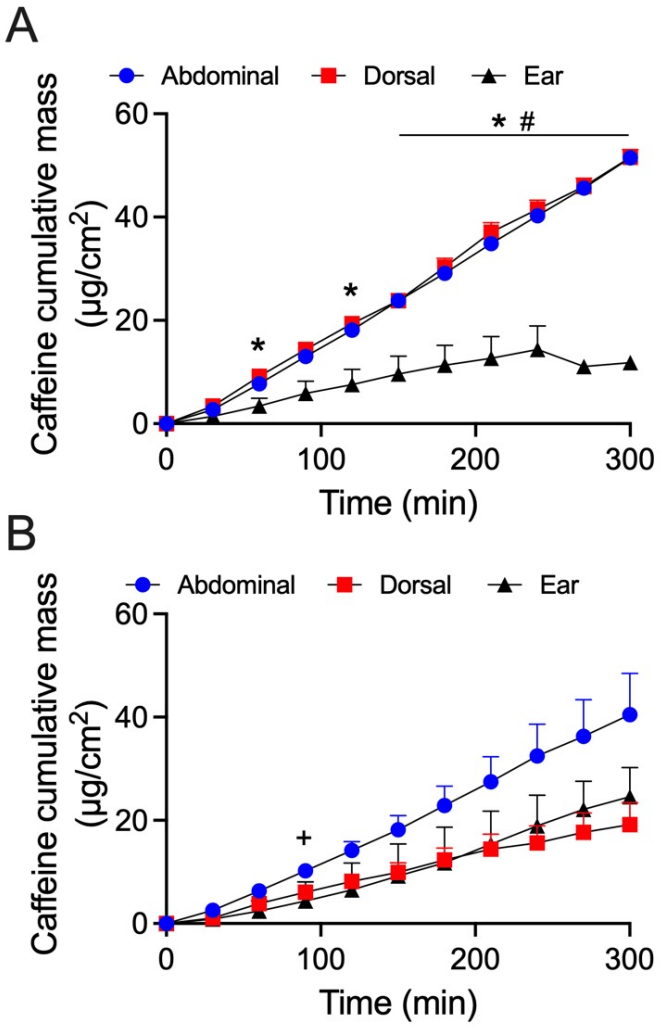

S3 Figure: Caffeine penetration through the skin at three different anatomical regions in (A) C57BL/6J mice, (B) SKH1

References

1. Rajkumar J, Chandan N, Lio P, Shi V (2023) The Skin Barrier and Moisturization: Function, Disruption, and Mechanisms of Repair. Skin Pharmacol Physiol, 36: 174–85.

2. Feingold KR (2007) Thematic review series: Skin Lipids. The role of epidermal lipids in cutaneous permeability barrier homeostasis. J Lipid Res, 48: 2531–46.

3. Iino Y, Naganuma T, Arita M (2023) Dysregulated ceramide metabolism in mouse progressive dermatitis resulting from constitutive activation of Jak1. J Lipid Res, 64: 100329.

4. Luo L, Guo Y, Chen L, Zhu J, Li C (2023) Crosstalk between cholesterol metabolism and psoriatic inflammation. Front Immunol, 14: 1124786.

5. Vaidya D, Ding J, Hill JG, Lima JAC, Crouse JR, Kronmal RA, et al. (2005) Skin tissue cholesterol assay correlates with presence of coronary calcium. Atherosclerosis, 181: 167–73.

6. Sprecher DL, Pearce GL (2005) Elevated skin tissue cholesterol levels and myocardial infarction. Atherosclerosis, 181: 371–3.

7. Robinson M, Visscher M, Laruffa A, Wickett R (2010) Natural moisturizing factors (NMF) in the stratum corneum (SC). I. Effects of lipid extraction and soaking. J Cosmet Sci, 61: 13–22.

8. Tang SC, Yang JH (2018) Dual Effects of Alpha-Hydroxy Acids on the Skin. Mol Basel Switz, 23: E863.

9. Piquero-Casals J, Morgado-Carrasco D, Granger C, Trullàs C, Jesús-Silva A, Krutmann J (2021) Urea in Dermatology: A Review of its Emollient, Moisturizing, Keratolytic, Skin Barrier Enhancing and Antimicrobial Properties. Dermatol Ther, 11: 1905–15.

10. Mojumdar EH, Pham QD, Topgaard D, Sparr E (2017) Skin hydration: interplay between molecular dynamics, structure and water uptake in the stratum corneum. Sci Rep, 7: 15712.

11. Asbóth D, Bánfi B, Kocsis D, Erdő F (2024) Rodent models of dermatological disorders. Ital J Dermatol Venereol, 159: 303–17.

12. The Jackson Laboratory. 000664 - B6 Strain Details [Internet]. C57BL/6J. (2023).

13. O'Neill SM, Brady MT, Callanan JJ, Mulcahy G, Joyce P, Mills KH, et al. (2000) Fasciola hepatica infection downregulates Th1 responses in mice. Parasite Immunol, 22: 147–55.

14. Rivera J, Tessarollo L (2008) Genetic Background and the Dilemma of Translating Mouse Studies to Humans. Immunity. 2008 Jan 18;28(1):1–4.

15. He X, Jia L, Zhang X (2022) The Effect of Different Preoperative Depilation Ways on the Healing of Wounded Skin in Mice. Animals, 12: 581.

16. Benavides F, Oberyszyn TM, VanBuskirk AM, Reeve VE, Kusewitt DF (2009) The hairless mouse in skin research. J Dermatol Sci, 53:10–8.

17. Schaffer BS, Grayson MH, Wortham JM, Kubicek CB, McCleish AT, Prajapati SI, et al. (2010) Immune Competency of a Hairless Mouse Strain for Improved Preclinical Studies in Genetically-Engineered Mice. Mol Cancer Ther, 9: 2354–64.

18. Horváth S, Komlódi R, Perkecz A, Pintér E, Gyulai R, Kemény Á (2019) Methodological refinement of Aldara-induced psoriasiform dermatitis model in mice. Sci Rep, 9: 3685.

19. Kocsis D, Horváth S, Kemény Á, Varga-Medveczky Z, Pongor C, Molnár R, et al. (2022) Drug Delivery through the Psoriatic Epidermal Barrier—A "Skin-On-A-Chip" Permeability Study and Ex Vivo Optical Imaging. Int J Mol Sci, 23: 4237.

20. Weber FC, Németh T, Csepregi JZ, Dudeck A, Roers A, Ozsvári B, et al. (2014) Neutrophils are required for both the sensitization and elicitation phase of contact hypersensitivity. J Exp Med, 212: 15–22.

21. Szederkényi G, Kocsis D, Vághy MA, Czárán D, Sasvári P, Lengyel M, et al. (2024) Mathematical modeling of transdermal delivery of topical drug formulations in a dynamic microfluidic diffusion chamber in health and disease. PLOS ONE, 19: e0299501.

22. Suzuki S, be K (1985) Topological structural analysis of digitized binary images by border following. Comput Vis Graph Image Process, 30: 32–46.

23. Lukács B, Bajza Á, Kocsis D, Csorba A, Antal I, Iván K, et al. (2019) Skin-on-a-Chip Device for Ex Vivo Monitoring of Transdermal Delivery of Drugs-Design, Fabrication, and Testing. Pharmaceutics, 11: E445.

24. Bajza Á, Kocsis D, Berezvai O, Laki AJ, Lukács B, Imre T, et al. (2020) Verification of P-Glycoprotein Function at the Dermal Barrier in Diffusion Cells and Dynamic 'Skin-On-A-Chip' Microfluidic Device. Pharmaceutics, 12: E804.

25. Varga-Medveczky Z, Kocsis D, Naszlady MB, Fónagy K, Erdő F (2021) Skin-on-a-Chip Technology for Testing Transdermal Drug Delivery-Starting Points and Recent Developments. Pharmaceutics, 13: 1852.

26. Herman A, Herman AP (2012) Caffeine's Mechanisms of Action and Its Cosmetic Use. Skin Pharmacol Physiol, 26: 8–14.

27. Bors L, Bajza Á, Kocsis D, Erdő F (2018) Caffeine: traditional and new therapeutic indications and use as a dermatological model drug. Orv Hetil, 159: 384–90.

28. Kocsis D, Kichou H, Döme K, Varga-Medveczky Z, Révész Z, Antal I, et al. (2022) Structural and Functional Analysis of Excised Skins and Human Reconstructed Epidermis with Confocal Raman Spectroscopy and in Microfluidic Diffusion Chambers. Pharmaceutics, 14: 1689.

29. Caspers PJ, Lucassen GW, Carter EA, Bruining HA, Puppels GJ (2001) In vivo confocal Raman microspectroscopy of the skin: noninvasive determination of molecular concentration profiles. J Invest Dermatol, 116: 434–42.

30. C57BL/6J Mice | Charles River (2023).

31. SKH1 Hairless Mouse | Charles River (2023).

32. Imhof RE, De Jesus MEP, Xiao P, Ciortea LI, Berg EP (2009) Closed-chamber transepidermal water loss measurement: microclimate, calibration and performance. Int J Cosmet Sci, 31: 97–118.

33. Rogiers V (2001) EEMCO Guidance for the Assessment of Transepidermal Water Loss in Cosmetic Sciences. Skin Pharma-

col Appl Skin Physiol, 14: 117–28.

34. Vater C, Apanovic A, Riethmüller C, Litschauer B, Wolzt M, Valenta C, et al. (2021) Changes in Skin Barrier Function after Repeated Exposition to Phospholipid-Based Surfactants and Sodium Dodecyl Sulfate In Vivo and Corneocyte Surface Analysis by Atomic Force Microscopy. Pharmaceutics, 13: 436.

35. Jain AK, Tewari-Singh N, Inturi S, Orlicky DJ, White CW, Agarwal R (2014) Histopathological and immunohistochemical evaluation of nitrogen mustard-induced cutaneous effects in SKH-1 hairless and C57BL/6 mice. Exp Toxicol Pathol, 66:129–38.

36. Goswami DG, Singh SK, Okoyeocha EOM, Roney AK, Madadgar O, Tuttle R, et al. (2024) Dermal Exposure to Vesicating Nettle Agent Phosgene Oxime: Clinically Relevant Biomarkers and Skin Injury Progression in Murine Models. J Pharmacol Exp Ther, 388:536–45.

37. Konger RL, Derr-Yellin E, Hojati D, Lutz C, Sundberg JP (2016) Comparison of the acute ultraviolet photoresponse in congenic albino hairless C57BL/6J mice relative to outbred SKH1 hairless mice. Exp Dermatol, 25: 688–93.

38. Köpf-Maier P, Mboneko VF, Merker HJ (1990) Nude Mice Are Not Hairless: A Morphological Study. Acta Anat (Basel), 139:178–90.

39. Massironi S, Giacóia MR, Maiorka P, Kipnis TL, Dagli M (2005) Skin morphology of the mutant hairless USP mouse. Braz J Med Biol Res Rev Bras Pesqui Médicas E Biológicas Soc Bras Biofísica Al, 38: 33–9.

40. Luo L, Lane ME (2015) Topical and transdermal delivery of caffeine. Int J Pharm, 490: 155–64.

41. van de Sandt JJM, van Burgsteden JA, Cage S, Carmichael PL, Dick I, Kenyon S, et al. (2004) In vitro predictions of skin absorption of caffeine, testosterone, and benzoic acid: a multi-centre comparison study. Regul Toxicol Pharmacol RTP, 39:271–81.

42. Salminen AT, Davis KJ, Felton RP, Nischal N, VonTungeln LS, Beland FA, et al. (2023) Parallel evaluation of alternative skin barrier models and excised human skin for dermal absorption studies in vitro. Toxicol In Vitro, 91:105630.

43. Otberg N, Patzelt A, Rasulev U, Hagemeister T, Linscheid M, Sinkgraven R, et al. (2008) The role of hair follicles in the percutaneous absorption of caffeine. Br J Clin Pharmacol, 65: 488–92.

44. Kocsis D, Klang V, Schweiger EM, Varga-Medveczky Z, Mihály A, Pongor C, et al. (2022) Characterization and ex vivo evaluation of excised skin samples as substitutes for human dermal barrier in pharmaceutical and dermatological studies. Skin Res Technol. 28: 664–76.

45. Lunter D, Klang V, Kocsis D, Varga-Medveczky Z, Berkó S, Erdő F (2022) Novel aspects of Raman spectroscopy in skin research. Exp Dermatol, 31: 1311–29.